AAS 15-253

PARTICLE AND MATCHED FILTERING USING ADMISSIBLE REGIONS

Timothy S. Murphy [*], Brien Flewelling[†], Marcus J. Holzinger [‡]

The main result to be presented in this paper is a novel matched filter based on orbital mechanics. The matched filter is an image processing technique which allows low signal-to-noise ratio objects to be detected. By using previous orbital knowledge, the matched filter utility can be increased. First, the particle filter implementation will be discussed followed by the implementation of the matched filter. Then a pair of simulation results will be presented, showing the results from the particle filter and matched filter.

INTRODUCTION

The Joint Space Operations Center (JSpOC) under U.S. Strategic Command operates The Space Surveillance Network (SSN) which tracks upwards of 17000 space objects of diameters greater than 10 cm.[1] The 2001 Rumsfeld Report stated a need for improved Space Situational Awareness (SSA) technologies to support US interests in space.[2] The SSN takes around 400,000 observations each day with radar, optical, and space based sensors.[1] Ground based optical sensors play a key role in tracking objects outside of Low Earth Orbit (LEO) where radar is less effective. It can also be seen as an affordable alternative to radar technologies.

The SSN includes both exquisite and minimalist sensors. Exquisite sensors have excellent noise characteristics enabling low magnitude object detection but often have a restrictive cost. Minimalist sensors focus on being cost-effective, allowing larger sensor networks but often lack the necessary noise requirements for detecting low magnitude objects. Sensors are also typically active, that is, able to track an objects through the sky. Tracking requires knowledge of the object's orbit. When orbit knowledge is poor or when discovering new objects, sensors must be passive, that is, fixed on a portion of the sky and imaging objects as they pass through the field of view. Discovering tracking, and determining orbits of low magnitude objects will continue to increase in importance. Exquisite sensors are needed to discover new objects, but are a limited resources. Minimalist sensors would be ideal for discovery and catalog upkeep. Passive sensing is needed for discovery and when tracking is impossible. The threshold for detection is signal-to-noise ratio (SNR), defined as the strength of a desired signal over the strength of noise present. This will be defined more rigorously in the Theory section. For tracking space objects (SO), SNR is the factor that limits an observer from seeing small or dim objects. This motivates processing techniques for enabling low SNR detection

[*] Graduate Student, The Guggenheim School of Aerospace Engineering, Georgia Institute of Technology, Georgia Institute of Technology North Ave NW, Atlanta, GA 30332.

[†] Research Aerospace Engineer, Space Vehicles Directorate, Air Force Research Laboratory, 3550 Aberdeen Ave. SE, Kirtland AFB, NM, USA.

[‡] Assistant Professor, The Guggenheim School of Aerospace Engineering, Georgia Institute of Technology, Georgia Institute of Technology North Ave NW, Atlanta, GA 30332. AIAA Senior Member

for passive sensors. The matched filter (MF) is an image filter which provides optimal SNR gain allowing images with low SNR to be useful, but requires prior knowledge of signal shape.

In current optical SSA applications, tracking, image processing, and orbit determination (OD) are often disjoint processes. In the tracking process, measurements are taken on an object without any online orbit update. Then, after tracking and data collection are complete, orbital parameters are estimated via a batch process or multiple hypothesis filter (MHF) type method. If the entire process of tracking, image processing, and OD are combined, there exist ways to improve these processing through feedback. This idea of feedback is what initially motivated an online matched filter.

The major result to be discussed in this paper is using results of online orbit determination to develop and apply an online matched filter (MF) primed by orbit knowledge and predicated on astrodynamics. The MF has been used in SSA applications but is limited by the requirement of known object shape.[3] The three dimensional MF was originally derived by Reed.[4] It is derived as a filter which provides an optimal SNR gain. The primary computation involved in a MF is image correlation. Correlation is a common process for feature detection in image processing.[5] A template is compared to all possible positions in an image and a value is assigned to each position. This value ranges from perfect correlation (1) to perfect anti-correlation (-1).

A common MF variation used in SO tracking is known as the velocity filter. A velocity filter uses knowledge of the velocity of an object in the image plane to approximate the streak that it should make. Under the assumption that no acceleration occurs in angle space, previous images can be correlated over future images to identify a SO. There are several limitations to this methodology. The primary limitation concerns the fact that any acceleration (in α and δ) of the object will change the streak from the template. This can be troublesome for an eccentric object or long integration times where accelerations are prevalent. A framework that provides online OD knowledge would enable a more sophisticated MF. This new MF is theoretically more robust to accelerations in the image plane which would be modeled by the dynamics This would also enable long propagation periods and can be transferred between geometrically diverse observers. In particular, the transfer between observers is interesting, as it allows exquisite sensors to pass off tracks to MF enabled minimal sensors. Additionally, minimal sensors could be enabled to perform catalog maintenance.

Admissible region (AR) theory will be used for the particle filter discussion and the matched filter results and is discussed here briefly. The AR as used for SO is based originally on work from Milani in the field of astrodynamics pertaining to heliocentric asteroids.[6] The work has since been adapted for SSA applications with much success.[7,8] As such, it is currently a hot topic and is expected to be a platform for a large number of novel research pathways. This paper will use the notation developed by Worthy et al.[9] for admissible regions. An AR is a set of ranges and range rates which corresponds to a particular angle and angle rate measurement. The AR is then constrained to a subset of ranges and range rates which correspond to physical orbits. Because the AR is an infinite set, the region often is sampled to create a discrete set of samples within the AR. These samples, also known as particles, can be used to prime numerous applications to carry out OD methods. A currently popular methodology is the Multiple Hypothesis Filter (MHF) proposed originally by DeMars, Jah, and Schumacher.[7] The principle behind MHF is that the samples from the admissible region can be thought of as hypothesis orbits. In an iterative scheme, these hypotheses are then filtered and pruned until a single or small set of orbits remain. This research will develop a particle filter (PF) to propagate forward and further constrain the orbit. The primary difference between MHF and a particle fitler is the way the orbits are modeled. Instead of considering samples to be disjoint hypotheses, a particle filter uses point wise discrete approximation for modeling. PF enables

the approximation of SO with non-Gaussian distributions based on orbital mechanics. Because this process includes an inherent resampling process, it is more robust to a sparse initial distribution. It should be noted that in practice, the MHF and PF are very similar being differentiated by only a sampling process.

Particle filters which are used for some of the results of this paper are discussed here. The particle filter has been used in orbital estimation scenarios in the past.[10] PF is typically considered to be one of the more accurate filtering methods when non-linear systems are involved.[11] True dynamics can be used to propagate forward particles instead of a linearized model, which increases fidelity. In the extended Kalman filter, which is typically used for non-linear systems, the filtered state is modeled as a Gaussian distribution. A particle filter models the filtered state as a non-Gaussian distribution as represented by a summation of Gaussian random variables called Virtual Particles (VP). There has been a push to move away from Gaussian distributions in OD techniques due to the highly non-Gaussian properties found in orbital element space.[12,13] This methodology, when applied correctly, can be a robust and effective method for determination of orbits with no restrictive Gaussian assumptions in the posterior distribution.

Typically, some type of filter is run on each of the VP in a particle filter. The Unscented Particle Filter (UPF) is a better suited method for nonlinear systems.[14] Particle filtering typically has large computational demands. One factor that mitigates this is that the unscented filtering process, which takes up the bulk of processing time, is highly parallelizable. The primary process is a propagator that must be run on each particle and all of their sigma points. In addition, a well designed PF operating on a "vaguely Gaussian" distribution can avoid the "curse of dimensionality".[15] The so-called "curse of dimensionality" in this case, refers to the fact that sampling an N dimensional space appropriately increases exponentially with respect to N. Because the mechanics involved in orbital mechanics a sufficiently non-linear and $N = 6$, particle filters have been historically avoided in OD. A second problem with particle filtering is choosing an appropriate prior distribution. The prior distribution is an initial choice of points to represent a distribution. Typically, proposal distribution is based on Sequential Importance Sampling, which approximates the distribution. AR solves both these problems by giving a new appropriate prior distribution based on the dynamics of the object, which can be sampled in a two dimensional space.

This paper will include discussions of admissible regions and particles filters, both of which are used to generate some of the results. The main contributions being presented here are: 1. The use of online orbital knowledge to prime a matched filter for initial orbit determination. 2. The use an admissible region to prime a matched filter bank for queued object detection. 3. The reduction of a matched filter bank computation time using admissible region discretization. This research is being incorporated as part of a larger software package, Generalized Electro-Optical DEtect Track Identify and Characterize Application (GEODETICA).

THEORY

Definition of Underlying Dynamics

First consider a space object, with position and velocity $\mathbf{r}$ and $\mathbf{v}$, seen by an optical observer at position and velocity $\mathbf{o}$ and $\dot{\mathbf{o}}$ along observation vector, $\boldsymbol{\rho}$. This is shown in Figure 1.

An optical measurement taken by an observer is a right ascension and declination and their rates. These have a one-to-one and onto transform to the observation unit vector and its rate of change, $\hat{\boldsymbol{\rho}}$ and $\dot{\hat{\boldsymbol{\rho}}}$. These are known states that can be represented as $\mathbf{x}_d = [\alpha \ \delta \ \dot{\alpha} \ \dot{\delta}]^T$. Then, the unknown

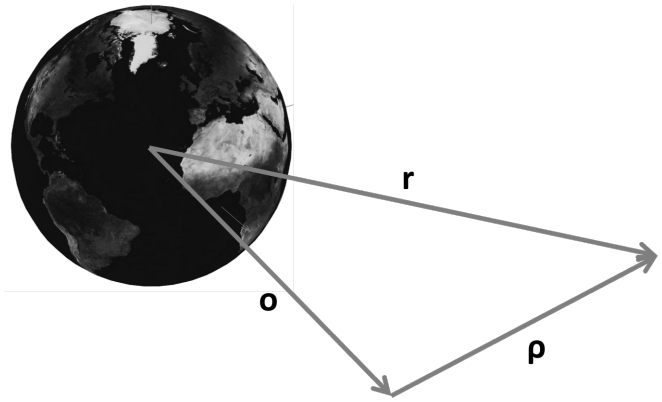

Figure 1: Setup of general observer problem.

states can be written as $\mathbf{x}_u = [\rho \;\; \dot{\rho}]^T$. The full state can then be written as

$$\mathbf{x} = \left[\mathbf{x}_d^T \;\; \mathbf{x}_u^T\right]^T \tag{1}$$

It is easy to see that a one-to-one and onto mapping, $\mathbf{m}$, exists between $\mathbf{x}$ and $\mathbf{x}_{ECI}(t) = [\mathbf{r}^T \;\; \mathbf{v}^T]^T$.

$$\mathbf{x} = \mathbf{m}(\mathbf{x}_{ECI}(t); \mathbf{k}) \tag{2}$$

where $\mathbf{k}$ is a parameter vector containing $\mathbf{o}$ and $\dot{\mathbf{o}}$. $\mathbf{k}$ is also time dependent but the explicit dependence will not be shown for convenience. Also note that $\mathbf{x}_{ECI}$ is assumed to be position and velocity but could also be written as orbital elements or any other full characterization of an orbit. The transform between these two is in essence a frame change between geocentric Cartesian frame and the observer-centric spherical frame. This mapping requires knowledge of $\mathbf{o}$ and $\dot{\mathbf{o}}$, assumed to be extremely well known, which for ground based observers is a good assumption. This paper will refer to $\mathbf{x}$ as the measurement frame and $\mathbf{x}_{ECI}$ as the Earth-centered inertial (ECI) frame.

This paper will also use the flow function to map $\mathbf{x}_{ECI}(t)$ through time.

$$\mathbf{x}_{ECI}(t) = \boldsymbol{\phi}(t, t_0, \mathbf{x}_{ECI}(t_0)) \tag{3}$$

Finally, define the following measurement function

$$\mathbf{y}(t) = \mathbf{h}_{ECI}(\mathbf{x}_{ECI}; k, t) \tag{4}$$

This also allows the definition of $\mathbf{H}(t)$, the Jacobian of the measurement function. Next, admissible regions will be explored.

Review of Admissible Regions for an Optical Observer

A typical optical measurement of a space object contains good knowledge of angle and angle rates known as observable states, $\mathbf{x}_d \in \mathbb{R}^4$. An orbit requires six disparate data types to be fully constrained. Historically, the final two data types are angle accelerations or range and range rate (from radar data). This AR formulation uses range and range rate as the final two states, known as undetermined states $\mathbf{x}_u \in \mathbb{R}^2$. It is assumed that no information can be reliably used to determine these states from measurements. The following notation was developed by Worthy et al.[9] Using equations (2) and (4) and the fact that the measurement cannot be dependent on $\mathbf{x}_u$, the following measurement function can be written.

$$\mathbf{y}(t) = \mathbf{h}(\mathbf{x}_d; \mathbf{k}, t) \tag{5}$$

Furthermore, this implies a one to one and onto relationship between $\mathbf{y}(t)$ and $\mathbf{x}_d$

$$\mathbf{x}_d = \mathbf{h}^{-1}(\mathbf{y}; \mathbf{k}, t) \tag{6}$$

An AR is then created by enforcing a series of constraints of the form

$$g_i(\mathbf{x}_d, \mathbf{x}_u; \mathbf{k}, t) \leqslant 0 \tag{7}$$

$$g_i(\mathbf{h}^{-1}(\mathbf{y}; \mathbf{k}, t), \mathbf{x}_u; \mathbf{k}, t) \leqslant 0 \tag{8}$$

It should be noted that these constraints can be thought of as hypotheses. The AR is then the space where all hypotheses are true. Next, we define an admissible region, $\mathcal{AR}_i \in \mathbb{R}^2$, predicated on g_i

$$\mathcal{AR}_i := \left\{\mathbf{x}_u | g_i(\mathbf{h}^{-1}(\mathbf{y}; \mathbf{k}, t), \mathbf{x}_u; k, t) \leqslant 0\right\} \tag{9}$$

In practice, an admissible region predicated on n constraints is used.

$$\mathcal{AR} = \bigcap_{i=1}^{n} \mathcal{AR}_i \tag{10}$$

Next, the two most common constraints are defined. For optical observer AR, the primary constraint typically considered is that of Earth-orbiting SO, defined as $g_{\mathcal{E}}$. There exists a derivation to show the following equations represent energy as a function of $[\rho, \dot{\rho}]$ and known parameters. The following results were originally derived for Earth objects by Tommei et al.[16] $\mathcal{E}$ is the orbital energy, which must be negative for an Earth-orbiting SO.

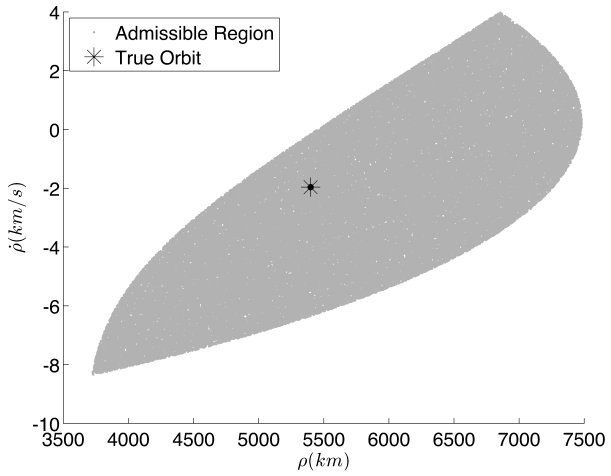

Figure 2: Sample admissible region based on energy and perigee constraints

$$2\mathcal{E} = g_{\mathcal{E}}(\mathbf{h}^{-1}(\mathbf{y};\mathbf{k},t),\mathbf{x}_u;\mathbf{k},t) \leqslant 0 \tag{11}$$

$$2\mathcal{E} = \dot{\rho}^2 + w_1\dot{\rho} + T(\rho) - \frac{2\mu}{\sqrt{S(\rho)}} \leqslant 0 \tag{12}$$

$$T(\rho) = w_2\rho^2 + w_3\rho w_4 \tag{13}$$

$$S(\rho) = \rho^2 + w_5\rho + w_0 \tag{14}$$

where the constants w_{0-5} are functions of the parameter vector, $\mathbf{k}$, defined as

$$w_0 = ||\mathbf{o}||^2 \tag{15}$$

$$w_1 = 2\dot{\mathbf{o}} \cdot \hat{\boldsymbol{\rho}} \tag{16}$$

$$w_2 = \dot{\alpha}^2 \cos^2\delta + \dot{\delta} \tag{17}$$

$$w_3 = 2(\dot{\alpha}\dot{\mathbf{o}} \cdot \hat{\boldsymbol{\rho}}_{\boldsymbol{\alpha}} + \dot{\delta}\dot{\mathbf{o}} \cdot \hat{\boldsymbol{\rho}}_{\boldsymbol{\delta}}) \tag{18}$$

$$w_4 = ||\dot{\mathbf{o}}||^2 \tag{19}$$

$$w_5 = 2\mathbf{o} \cdot \hat{\boldsymbol{\rho}} \tag{20}$$

where $\mathbf{o}$ and $\dot{\mathbf{o}}$ are the position and velocity of the observer, $\hat{\boldsymbol{\rho}}$ is the unit vector from the angles, and $\hat{\boldsymbol{\rho}}_\alpha$ and $\hat{\boldsymbol{\rho}}_\delta$ are given by

$$\hat{\boldsymbol{\rho}} = [\cos\alpha\cos\delta \;\; \sin\alpha\cos\delta \;\; \sin\delta]^T \tag{21}$$

$$\hat{\boldsymbol{\rho}}_{\boldsymbol{\alpha}} = [-\sin\alpha\cos\delta \;\; \cos\alpha\cos\delta \;\; 0]^T \tag{22}$$

$$\hat{\boldsymbol{\rho}}_{\boldsymbol{\delta}} = [-\cos\alpha\sin\delta \;\; -\sin\alpha\sin\delta \;\; \cos\delta]^T \tag{23}$$

A second commonly used constraint is g_r, a constraint on the radius of perigee. There exists a analytic derivation for the following.[17] It should be noted that **D**, **E**, **F**, and **G** are vector quantities.

$$g_r(\rho, \dot{\rho}, \mathbf{x}_d; \mathbf{k}) = (r_{min}^2 - \|\mathbf{D}\|^2)\dot{\rho} - P(\rho)\dot{\rho} - U(\rho) + r_{min}^2 T(\rho) - \frac{2r_{min}\mu}{\sqrt{S(\rho)}} \leqslant 0 \tag{24}$$

$$P(\rho) = 2\mathbf{D}\cdot\mathbf{E}\rho^2 + 2\mathbf{D}\cdot\mathbf{F}\rho + 2\mathbf{D}\cdot\mathbf{G} - r_{min}^2 w_1 \tag{25}$$

$$U(\rho) = \|\mathbf{E}\|^2\rho^4 + 2\mathbf{E}\cdot\mathbf{F}\rho^3 + (2\mathbf{E}\cdot\mathbf{G} + \|\mathbf{F}\|^2)\rho^2 + 2\mathbf{F}\cdot\mathbf{G}\rho + \|\mathbf{G}\|^2 - 2r_{min}\mu \tag{26}$$

where the **D**, **E**, **F**, and **G** are defined as

$$\mathbf{D} = \mathbf{q} \times \hat{\boldsymbol{\rho}} \tag{27}$$

$$\mathbf{E} = \hat{\boldsymbol{\rho}} \times (\dot{\alpha}\hat{\boldsymbol{\rho}}_\alpha + \dot{\delta}\hat{\boldsymbol{\rho}}_\delta) \tag{28}$$

$$\mathbf{F} = \mathbf{q} \times (\dot{\alpha}\hat{\boldsymbol{\rho}}_\alpha + \dot{\delta}\hat{\boldsymbol{\rho}}_\delta) + \hat{\boldsymbol{\rho}} \times \dot{\mathbf{q}} \tag{29}$$

$$\mathbf{G} = \mathbf{q} \times \dot{\mathbf{q}} \tag{30}$$

More ways exist to further constrain an admissible region. Beyond perigee and energy, any further restriction typically requires an assumption about the object. For example, if the object being observed is known to be near a GEO, constraints could be placed on semi major axis or eccentricity. This can enable prior orbital knowledge to be used to enhance convergence.

Particle Filter Process

The following discussion assumes that some parallel algorithm is running to make associations and obtain measurements. While the particle filtering methodology can be used for data association, it fails to have any utility over a more typical method and has computational restrictions. An initial measurement is used to create an AR. Note that this requires angles and angle rates, which can be obtained from a single measurement with sufficient exposure. However, more measurements can lead to more accurate initial measurements and therefore is recommended. The AR is sampled through some methodology which could include but is not limited to random sampling, some predetermined grid, Delauney triangulation, or Gaussian mixture models. In general, an even spacing of points within the AR is desirable.[6,7] An evenly spaced distribution in the AR can be mapped into another space, such as postion and velocity, and used as a prior distribution for a particle filter. The process is shown in Figure 3, along with what uses the output of the PF. The output can be used to enable a matched filter or sensor tasking.

For each iteration of the particle filter, the following occurs: A new measurement at a future time is obtained. Each particle is then run through one iteration of an unscented Kalman filter[14] using this new measurement to update. The updated VP are then compared to the measurement via a multivariate Gaussian distribution. A weight, w_k, is then updated as the product of the previous weight and the new probability. This allows time history to be incorporated into the weights.

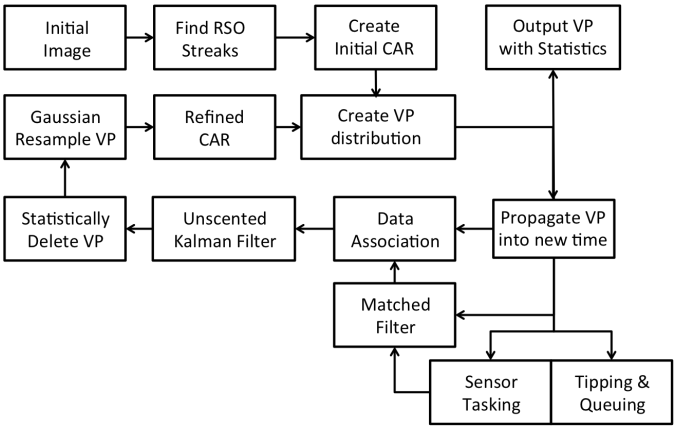

Figure 3: Particle filter process with relevant outputs

$$p(\mathbf{z}_k|\mathbf{x}_{k-1}^i) = \frac{1}{\sqrt{(2\pi)^l|\mathbf{P}_k|)}} \exp\left(-\frac{1}{2}(\mathbf{x}_k^i - \mathbf{z}_k)\mathbf{P}_k^{i,-1}(\mathbf{x}_k^i - \mathbf{z}_k)^T\right) \tag{31}$$

$$\mathbf{P}_k^i = \mathbf{R}_k + \mathbf{H}(t_k)\mathbf{P}^i(t_k)\mathbf{H}(t_k) \tag{32}$$

$$w_k^i = w_{k-1}^i p(\mathbf{z}_k|\mathbf{x}_{k-1}^i) \tag{33}$$

where the measurement has l dimensions, $\mathbf{x}_k^i$ is the i^{th} VP at time step k, mapped into the measurement space, $\mathbf{z}_k$ is the new measurement at timestp k, $\mathbf{R}_k$ is the measurement noise covariance at time step k, $\mathbf{P}^i(t_k)$ is the covariance of a the i^{th} VP, and w_k^i is the weight assigned to the i^{th} particle at time step k. The weights are then renormalized such that the total distribution sums to 1.

VP deleting and resampling occur next. A threshold is set to determine which particles to delete. When $w_k^i < w_{min}$ is satisfied, a particle is deleted. The threshold is highly dependent on the desired distribution size; larger distributions require lower thresholds. Resampling occurs when the number of particles falls below a certain threshold at which point it is considered too few particles to accurately represent the distribution. Each particle is resampled based on the following

$$N_k^i = \frac{w_k^i}{C} \tag{34}$$

where N_k^i is the number of new VP to be sampled from the i^{th} parent VP, w_k^i is the current weight for the i^{th} VP, and C is some given threshold based on the size of the desired distribution. N^i is rounded down, and N^i new VP are sampled from the Gaussian distribution of the i^{th} VP. Note that this assures that no current VP is deleted but instead only new VP are created. Finally, the weights, $w_{k,new}^i$ of the newly sampled VP are renormalized based on the parent VP weight, w_k^i, by making each VP weight the following

$$w_{k,new}^i = \frac{w_k^i}{N_k^i + 1} \tag{35}$$

This is also done for the parent particle, ensuring no total rise in probability has occurred. The two threshold parameters, w_{min} and C warrant further discussion. Both parameters are chosen

primarily to maintain a certain distribution size. The number of VP is not fixed, but instead varies over time as VP are deleted and resampled.

Orbital Mechanics Enabled Matched Filter

Matched Filter Background

Matched filtering originates in image processing and signal processing as an optimal method for signal detection. The original formulation dates back to the 1960s as a way to optimally detect a signal in a high noise environment.[18] It was then adapted to general image processing and moving target detection.[4]

First, define a measurement as $\mathbf{Y}(t) \in \mathcal{Y}$ which could be a scalar, vector or matrix. $\mathbf{Y}(t)$ can be broken into a meaningful signal $\mathbf{S}(t) \in \mathcal{Y}$ and a Gaussian white noise signal as $\mathbf{W}(t) \in \mathcal{Y}$. Additionally, assume that template $\mathbf{S}_0(t) \in \mathcal{T}$ is known and its signal shape matches $\mathbf{S}(t)$. A matched filter can then be defined as a mapping $f_{MF}(t) : \mathcal{Y} \times \mathcal{T} \rightarrow \mathcal{Y}$

$$\mathbf{Y}(t) = \mathbf{S}(t) + \mathbf{W}(t) \tag{36}$$

$$\mathbf{Y}'(t) = f_{MF}(\mathbf{Y}(t), \mathbf{S}_0(t)) \tag{37}$$

Note that $\mathcal{T} \subset \mathcal{Y}$ such that $\mathbf{S}_0(t)$ is smaller than $\mathbf{Y}(t)$. $\mathbf{S}_0(t)$ is matched over every spot in $\mathbf{Y}(t)$ and a correlation result is formed. $\mathbf{Y}'(t)$ is then the result of correlating $\mathbf{S}_0(t)$ with every location in $\mathbf{Y}(t)$. The SNR of $\mathbf{Y}(t)$ and $\mathbf{Y}'(t)$ at a certain coordinate $\mathbf{z}$ are defined as:

$$SNR_{Y,z} = \frac{\mathbb{E}[\mathbf{Y}(\mathbf{z},t)]^2}{\mathbb{E}[(\mathbf{Y}(\mathbf{z},t) - \mathbb{E}[\mathbf{Y}(\mathbf{z},t)])^2]} \tag{38}$$

$$SNR_{Y',z} = \frac{\mathbb{E}[\mathbf{Y}'(\mathbf{z},t)]^2}{\mathbb{E}[(\mathbf{Y}'(\mathbf{z},t) - \mathbb{E}[\mathbf{Y}'(\mathbf{z},t)])^2]} \tag{39}$$

It has been shown that the correlation based filter which is predicated on an accurate template at the correct coordinate, will produce an optimal SNR gain $K_{SNR} = SNR_{Y',z}/SNR_{Y,z}$.[19] This problem is solved and built into MATLAB, making implementation of an MF simple. A good discussion of this with respect to optical systems is presented by Dragovic.[3] The utility of the MF is enabling low SNR measurements in $\mathbf{Y}(s)$ to be used if the signal shape is known.

When applied to the general tracking problem, MF typically takes the form of a velocity filter (VF).[20] The VF uses the assumption that an object, moving through an image plane, has constant velocity between measurements. This allows previous measurements to act as templates for future images. Over short periods of time this assumption is typically good and VF work well. Another method relies on a bank of matched filters varying over a range of velocities, attempting to improve robustness at the expense of computation. The assumption of constant velocity is dependent on the type of orbit being examined and with sufficient time will become prohibitive. The limitations of the VF is the inability to operate outside of high frequency measurements from the same observer.

Matched Filter Primed by Previous Orbital Knowledge

The first contribution of this paper is proposing a MF for orbital tracking applications which does not require a constant velocity assumption. Assume there exists a state probability density

function (PDF) of a SO, $f(\mathbf{x}_{ECI}(t))$, in the ECI frame. This distribution can then be mapped to the measurement frame of the i^{th} observer

$$f(\mathbf{x}_i(t)) = f(\mathbf{m}_i(\mathbf{x}_{ECI}(t))) \tag{40}$$

This distibution can also be mapped forward in time using the known flow function.

$$f(\mathbf{x}_i(t)) = f(\mathbf{m}_i(\boldsymbol{\phi}(t, t_o, \mathbf{x}_{ECI}(t_o)))) \tag{41}$$

By varying t, a single point in $f(\mathbf{x}_{ECI}(t))$ can be mapped over the integration time of an observer. The mean or a VP sampled from the distribution could be used as a representative orbit. A representative orbit can then be mapped through an integration time, to form an arc through space. The collinearity equations or another sensor model can be used to map a point or arc in space into an optical sensor image frame.[21] This process allows the simulation of a measuremnt image, which can be used as $\mathbf{S}_0(t)$.

This MF has no assumptions about previous measurements. Unlike a velocity filter, the proposed MF can freely switch between observers or operate over large times between observations. There exists some limitations. The proposed MF is predicated on good orbital knowledge of the SO, that is, $f(\mathbf{x}_{ECI})$ is sufficiently small. If $f(\mathbf{x}_{ECI})$ is an excellent representation of a SO, many sensors are able to rate track objects of interest. Passive sensors do not require excellent orbital knowledge, but are seldom used. This methodology would be useful for passive sensors and could enhance the utility of passive sensing. More important, object discovery also motivates use of a MF, in which dim objects are discovered but cannot be yet tracked.

Matched Filter Primed by Single Observation

Next, the previous result will be applied to the case of a single measurement as the only prior knowledge. It is useful to define a second measurement space incorporating integration time, t_{int}. By calculating, $\mathbf{m}_i(\mathbf{x}_{ECI}(t_0))$ and $\mathbf{m}_i(\boldsymbol{\phi}(t_0 + t_{int}, t_0, \mathbf{x}_{ECI}(t_0)))$, the angular rate heading, ϕ_a and magnitude, v_a, can be determined. This paper will define $v_a = ||[\dot{\alpha}, \dot{\delta}]^T||, \phi_a = atan(\frac{\dot{\delta}}{\dot{\alpha}})$. However, ϕ_a and v_a could be defined in terms of the observer orientation. Defining $\mathbf{x}_{v,\phi} = [v_a, \phi_a]^T$, the following projection will be defined for observer i

$$\mathbf{x}_{v,\phi;i} = \mathbf{p}_i(t_0, t_{int}, \mathbf{x}_{ECI}(t_0), \mathbf{k}) \tag{42}$$

This projection can be thought of as sensor model for an observer, allowing the projection of a the beginning and end of a streak into the sensor frame. Projecting into angle space, and defining rates in terms of right ascension and declination can also be used. This new space is useful because $\mathbf{x}_{v,\phi}$ fully defines the shape of a measurement, which is all that is needed to define $\mathbf{S}_o$. It should be noted that using $\mathbf{x}_{v,\phi;i}$ assumes no angular acceleration over the course of t_{int}. This is justified if t_{int} is sufficiently small.

An admissible region, $\mathcal{AR}$, can be created for the SO from a measurement from observer i. $\mathcal{AR}$ can be used to create a uniform PDF over all possible $\mathbf{x}_u(t)$, which will be called $f_i(\mathbf{x}(t))$. Next consider the following mapping

$$f_{v,\phi;j}(\mathbf{x}_{v,\phi}(t_1)) = f(\mathbf{p}_j(t_1, t_{int}, \boldsymbol{\phi}(t_1, t_0, m_i^{-1}(\mathbf{x}(t_0)))))) \tag{43}$$

$\mathbf{f}_{v,\phi;j}(\mathbf{x}_{v,\phi}(t_1))$ is the $\mathcal{AR}$ PDF mapped forward in time and to a second observer. At this point, there exist multiple methods for creating a useful MF template. An point-wise discrete approximation can be used to represent $\mathcal{AR}$ with n VP. These VP can be mapped through (43). n templates can be created and tested on a new measurement. Each template can be correlated with the new measurement in the form of a bank of MF. If the point-wise discretization is sufficiently dense, then at least one of the templates created will have optimal SNR gain in the form of an ideal MF. Many VP should not exhibit high SNR gain with the new measurement. This is analogous to a PF weight update, and could have utility, but will not be further analyzed here. High correlation can be used to obtain a new measurement, which is the goal of the MF. It should be noted that this assumes measurement noise in the initial observation is accounted for, but there has been recent work in this area.[9]

A single MF requires generation of a template, and a correlation over the entire measurement. A bank of n MF may be prohibitively costly for online measurements. $\mathcal{AR}$ is a connected set which is mapped through multiple continuous transformations. If a subset, $\mathcal{S}_k \subset \mathcal{AR}$, which is connected and sufficiently small is mapped to $\mathbf{f}_{v,\phi}$, it will remain connected and small. This implies that any VP within an intelligently chosen $\mathcal{S}_k$ will produce effectively equivalent templates. By creating s subsets with the following restriction

$$\mathcal{AR} = \bigcup_{k=1}^{s} \mathcal{S}_k \tag{44}$$

$\mathcal{AR}$ can be partitioned. The partitioning is designed by instead partitioning $\mathbf{f}_{v,\phi;j}(\mathbf{x}_{v,\phi}(t_1))$. By grouping regions in $\mathbf{f}_{v,\phi;j}(\mathbf{x}_{v,\phi}(t_1))$ into partitions of similar $\mathbf{x}_{v,\phi}$, subsets $\mathcal{S}_{v,\phi;k}$ can be created to contain all similar templates. Each subset, $\mathcal{S}_{v,\phi;k}$, can be mapped through the inverse of (43), allowing $\mathcal{S}_k$ to be defined. How subsets of $\mathbf{f}_{v,\phi;j}$ can be chosen is dependent on what makes template similar enough. One method which will be used to simulate results in this paper is a partition grid by choosing limits in difference of both v_a and ϕ_a. This will reduce the number of templates from n to s.

SIMULATION & RESULTS

Particle Filter

To demonstrate the effectiveness of the PF, a simulation was run of a GEO object in a circular orbit. The observer is a ground-based optical observer. Observations are taken every 2 minutes by the same observer. The true orbit has a semi major axis of 42,164 km and an effective eccentricity of zero.

In Figure 4, the resulting PDF is shown at 0, 30, and 60 minutes of observation. The orientation of the orbit must also be determined but is difficult to visualize. For this reason, the PDF is plotted only in semi major axis and eccentricity which define the shape of the orbit. This allows the convergence to be visualized easily. At $t = 0$, the result is equivalent to the initial AR, that is, it is the full range of orbits for that particular initial observation. At $t = 30, 60$ min, convergence continues to improve.

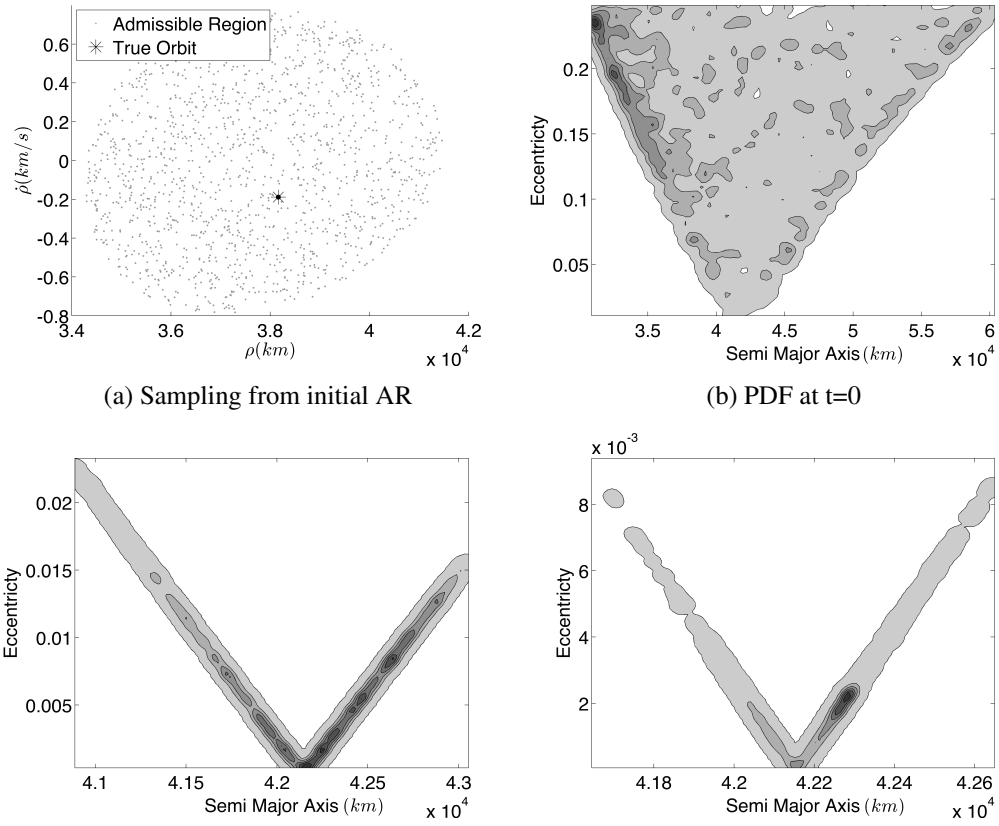

(a) Sampling from initial AR

(b) PDF at t=0

(c) PDF at 30 minutes

(d) PDF at 60 minutes

Figure 4: Results from particle filter

The initial samples drawn from the AR are shown in Figure 4 as well. A restriction was placed on eccentricity during the initial sampling. The smaller distribution allows better visualization early on, but the final results would be the same with no restriction.

Matched Filter

Matched Filter Based on Orbital Mechanics

In Figure 5, the results of a simulated object in a simulated observer's image plane is shown. The first frame has no noise, showing what the measured signal over a certain exposure, $\mathbf{S}(t_k)$, looks like. The second frame is the measurement as seen by an observer, $\mathbf{Y}(t_k)$, with noise. This image has a SNR of approximately $SNR_{Y,z} = 0.5$. The third frame has the correlation result, $\mathbf{Y}'(t_k)$, ranging from white (perfect correlation) to black (perfect anti-correlation). The template, $\mathbf{S}_o(t_k)$, is also shown. The correlation results SNR, $SNR_{Y',z}$, is difficult to calculate as it is requires separating the signal and the noise, $\mathbf{S}(t)$ and $\mathbf{W}(t)$ or a Monte Carlo. The gain is visible in Figure 5. There is a clear visible peak in $SNR_{Y',z}$ that is not present in $SNR_{Y,z}$. This verifies that the proposed MF can be used as proposed, and also illustrates the type of results provided by the MF.

(a) Simulated streak without noise ($\mathbf{S}(t)$)

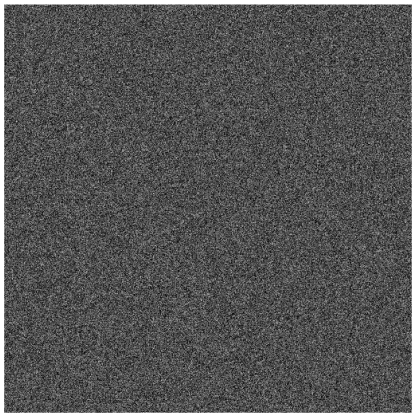

(b) Simulated measurement with noise ($\mathbf{Y}(t)$)

c

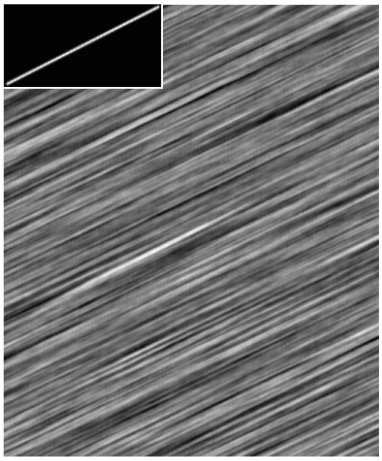

(c) Correlation result ($\mathbf{Y}'(t)$)

Figure 5: Results from matched filter

Matched Filter Bank

A simulation is shown in Figure 6 to validate the proposed matched filter bank. An unknown SO has a single observation taken on it by an optical observer in Colorado at $t = 0$. An AR is created based on the observation, propagated forward in time by 60 seconds, and projected into the view of a second optical observer at Hawaii. Each particle is used to create a streak, all of which are used to create a histogram in terms of streak length and orientation. These mappings are equivalent to (43). These streaks are partitioned into discrete subsets at intervals of one degree in heading and pixel size in streak length. The total PDF and the partitions can be seen in Figure 6. Approximately 100 partitions were needed to generate templates, $\mathbf{S}_{o,1} - \mathbf{S}_{o,100}$. Each template is correlated against the new measurement, $\mathbf{Y}(t = 60)$. The results are plotted in terms of peak correlation, shown in Figure 6. The correlation SNR, $SNR_{Y',z}$, and SNR gain are direct functions of the peak correlation. These correlations allow the streak to be identified within the image.

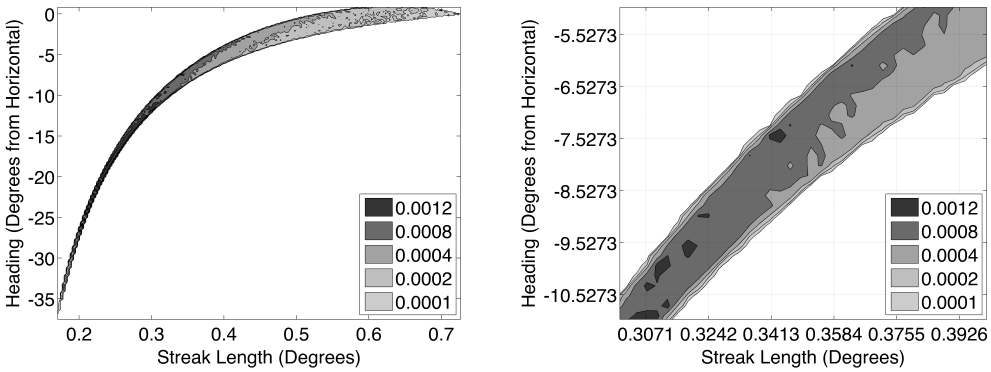

(a) Entire PDF

(b) Zoom in with discretization

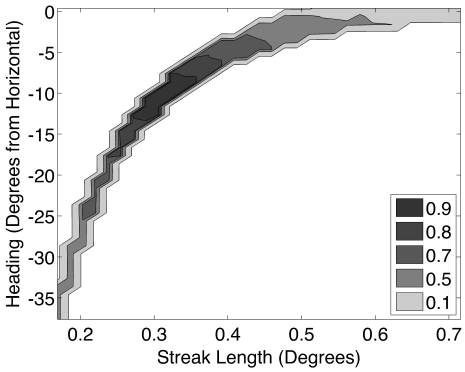

(c) Correlation results from matched filter bank

Figure 6: PDF of streaks predicted by admissible region in terms of v, ϕ

CONCLUSION

Admissible regions and particle filtering have been discussed. The proposed matched filter has been developed as an effective method for enabling passive sensors to take low SNR measurements. This matched filter is an improvement over velocity filters by the incorporation of orbital mechanics. This has also been built into the framework of detection of new SO and sensor hand off. A discretization method has been proposed for partitioning a discrete point-wise prior distribution for efficient computation time.

ACKNOWLEDGMENT

We would like to acknowledge and thank the Air Force Research Laboratory Space Scholars Program for supporting this project. Finally, we would like to extend thanks to Brad Sease for aiding the development of this project.

REFERENCES

[1] "spacetracks.org," December 2014.

[2] D. Rumsfeld, D. Andrews, R. Davis, H. Estes, R. Fogleman, J. Garner, W. Graham, C. Horner, D. Jeremiah, T. Moorman, *et al.*, "Report of the Commission to Assess United States National Security Space Management and Organization," tech. rep., 2001.

[3] M. Dragovic, *Velocity filtering for target detection and track initiation*. PhD thesis, 2003.

[4] I. Reed, R. Gagliardi, and H. Shao, "Application of three-dimensional filtering to moving target detection," *Aerospace and Electronic Systems, IEEE Transactions on*, No. 6, 1983, pp. 898–905.

[5] R. C. Gonzalez and R. E. Woods, "Digital imaging processing," *Massachusetts: Addison-Wesley*, 1992.

[6] A. Milani, G. F. Gronchi, M. d. Vitturi, and Z. Knežević, "Orbit determination with very short arcs. I admissible regions," *Celestial Mechanics and Dynamical Astronomy*, Vol. 90, No. 1-2, 2004, pp. 57–85.

[7] K. J. DeMars, M. K. Jah, and P. W. Schumacher, "Initial orbit determination using short-arc angle and angle rate data," *Aerospace and Electronic Systems, IEEE Transactions on*, Vol. 48, No. 3, 2012, pp. 2628–2637.

[8] K. Fujimoto and D. Scheeres, "Correlation of optical observations of earth-orbiting objects and initial orbit determination," *Journal of guidance, control, and dynamics*, Vol. 35, No. 1, 2012, pp. 208–221.

[9] J. L. Worthy III and M. J. Holzinger, "Incorporating Uncertainty in Admissible Regions for Uncorrelated Detections Incorporating Uncertainty in Admissible Regions for Uncorrelated Detections Incorporating Uncertainty in Admissible Regions for Uncorrelated Detections Incorporating Uncertainty in Admissible Regions for Uncorrelated Detections," *AIAA/AAS Astrodynamics Specialist Conference*, 2014.

[10] G. Wang and X.-j. Duan, "Particle filtering and its application in satellite orbit determination," *Image and Signal Processing, 2008. CISP'08. Congress on*, Vol. 5, IEEE, 2008, pp. 488–492.

[11] H. Chen, G. Chen, E. Blasch, and K. Pham, "Comparison of several space target tracking filters," *SPIE Defense, Security, and Sensing*, International Society for Optics and Photonics, 2009, pp. 73300I–73300I.

[12] K. Vishwajeet, P. Singla, and M. Jah, "Nonlinear Uncertainty Propagation for Perturbed Two-Body Orbits," *Journal of Guidance, Control, and Dynamics*, 2014, pp. 1–11.

[13] K. J. DeMars and M. K. Jah, "Probabilistic initial orbit determination using gaussian mixture models," *Journal of Guidance, Control, and Dynamics*, Vol. 36, No. 5, 2013, pp. 1324–1335.

[14] R. Van Der Merwe, A. Doucet, N. De Freitas, and E. Wan, "The unscented particle filter," *NIPS*, 2000, pp. 584–590.

[15] F. Daum and J. Huang, "Curse of dimensionality and particle filters," *Aerospace Conference, 2003. Proceedings. 2003 IEEE*, Vol. 4, IEEE, 2003, pp. 4_1979–4_1993.

[16] G. Tommei, A. Milani, and A. Rossi, "Orbit determination of space debris: admissible regions," *Celestial Mechanics and Dynamical Astronomy*, Vol. 97, No. 4, 2007, pp. 289–304.

[17] D. Farnocchia, G. Tommei, A. Milani, and A. Rossi, "Innovative methods of correlation and orbit determination for space debris," *Celestial Mechanics and Dynamical Astronomy*, Vol. 107, No. 1-2, 2010, pp. 169–185.

[18] D. O. North, "An analysis of the factors which determine signal/noise discrimination in pulsed-carrier systems," *Proceedings of the IEEE*, Vol. 51, No. 7, 1963, pp. 1016–1027.

[19] G. L. TURINT, "An introduction to matched filters," 1960.

[20] P. F. Singer, "Performance analysis of a velocity filter bank," 1997, pp. 96–107.

[21] J. L. Crassidis and J. L. Junkins, *Optimal estimation of dynamic systems*. CRC press, 2011.